A high-fidelity simulation model for the precise characterization of a solar air-cooled ammonia-water absorption chiller at part load operation

María Esther Palacios-Lorenzo[a], José Daniel Marcos[a]

[a]*Dept. of Energy Engineering, UNED, Madrid, Spain, epalacios@ind.uned.es*

Abstract:

A differential mathematical model has been developed for the simulation of the ammonia-water absorption refrigeration system ROBUR®, model ACF60-00 LB. The model, with modular structure, contains the governing equations based on mass, species, and energy, implemented for the main system components. The model captures both thermal and mass resistance in the mass and transfer processes that simultaneously occur in the system. A calculation procedure is presented to evaluate the performance of the cooling system under off-design conditions, when driven by hot water temperature ranging between 160 and 210 ºC. Performance of the system when the ambient temperature is up to 40ºC has been analysed, assumed that the pumped solution flow rate kept constant, and the high-pressure level may be used as a control strategy. Results show that, at ambient temperature of 40ºC, the cooling capacity of the is restricted by the size of the air-coolant absorber if the feed hot water temperature is 210ºC. However, difficulties in condenser operation reduce the cooling capacity of the system when the temperature of the feed water drops to 160ºC. In addition, at ambient temperature of 40ºC and feed water temperature of 210ºC, geometry restriction due to the rectifier and the solution-cooled absorber results in COP increase. In such working conditions, the refrigeration system operates at its maximum high-pressure level.

Keywords:

Thermodynamics; ammonia-water; hot climate; absorption; GAX; ASTEP

1. Introduction

The world's population is expected to reach 9,7 billion people in 2050 [1]. Population growth beside economic development and changing consumption pattern will be followed of a notable increase in energy and water consumption. Therefore, there is a greater concern to reduce the environmental impact of energy and to optimize the efficient use of water. Currently, there is a great deal of interest in absorption systems because of their environmentally friendly technology. Absorption systems can help to reduce CO_2 emissions, slowing global warming and biodiversity loss. One of the main advantages of absorption systems is the possibility of using both waste heat from industrial processes and solar energy as a power source. In addition, absorption systems when air-cooled have no water consumption.

In this framework, the European ASTEP project has, among other main goals, to demonstrate the feasibility of the application of solar thermal energy to partially cover the cooling demands at an industrial site. Specifically, one of the tasks is partially satisfy the MANDREKAS dairy company cooling demand, at 5ºC, at different operating conditions, such as feed hot water temperature and outdoor temperature. Feed hot water temperature is supplied by a patented solar concentrator (sun dial).

The ammonia-water mixture is particularly suitable for generating chilled water at sub-zero temperatures in air-cooled systems. The most relevant drawback of the ammonia-water mixture, which determines the operation of the absorption systems, is that the vapor pressure of the water is not negligible as compared to the vapor pressure of the ammonia. As a result, the refrigerant always contains a small amount of water. The presence of water in the evaporator significantly deteriorates the performance and the efficiency of the system. The water content in the refrigerant can be reduced by using a distillation column [2]-[3], a condensation rectifier [5]. The efficiency of the system may be improved when the absorption system operates according to a GAX cycle. The key problem in the GAX cycle is the heat transfer between the absorber and the generator [6].

In the present analysis, a differential mathematical model with modular structure has been developed. The model implemented is based on the equations developed by Colburn and Drew for the condensation of a binary vapor mixture with a miscible condensate, [7]. The model includes the mass transfer resistance in both the liquid and vapor phases, which is dominant in the mass transfer processes occurring in an absorber system

https://doi.org/10.52202/069564-0081

[8]. The discretized and modular character of the model together with the consideration of mass transfer resistances gives it a high reliability. The model studies the performance and efficiency of the ammonia-water absorption refrigeration system ROBUR®, model ACF60-00 LB, at part load operation, focusing on the operating condition in hot climate when driven with hot water at high and low temperature. Limitations in the operation of the chiller to ambient temperature beyond 40ºC are analysed.

2. Methodology

2.1 System description

To study the performance of the single effect air-cooled ammonia/water absorption chiller, a mathematical model has been implemented in Engineering Equation Solver Software, on the bases of mass, species and energy conservation balances. The material thermal properties have been evaluated from [9]. Figure 1 shows a schematic diagram of the chiller. The geometry of the different devices of which the chiller consists, are detailed in Table 1. The distillation column includes a rectifying section and a stripping section, located respectively, above and below of the column feed entry point. A rectifier completes the purification system to achieve vapor refrigerant with a high grade of purity. The lack of appreciable benefits that the rectifying section entails, beside the decrease of COP associated with the use of coupled fluid-cooled rectifier [2]-[3] justifies considering the purifying system to consist of a distillation column fed from above (only with striping section) helped by a concentrated solution-cooled rectifier to obtain refrigerant vapor of the required purity. This assumption is corroborated by the schematic diagram of the ROBUR [10]-[11]. An solution-cooled absorber operates as regenerative generator absorption heat chiller, GAX [12]. The chiller includes three restrictors. Restrictors 2 and 3 allow to reestablish the low-pressure level at the inlet of the solution pump. In this study, it is assumed that restrictor 1 allows regulate both high- and low-pressure levels to optimize the chiller performance.

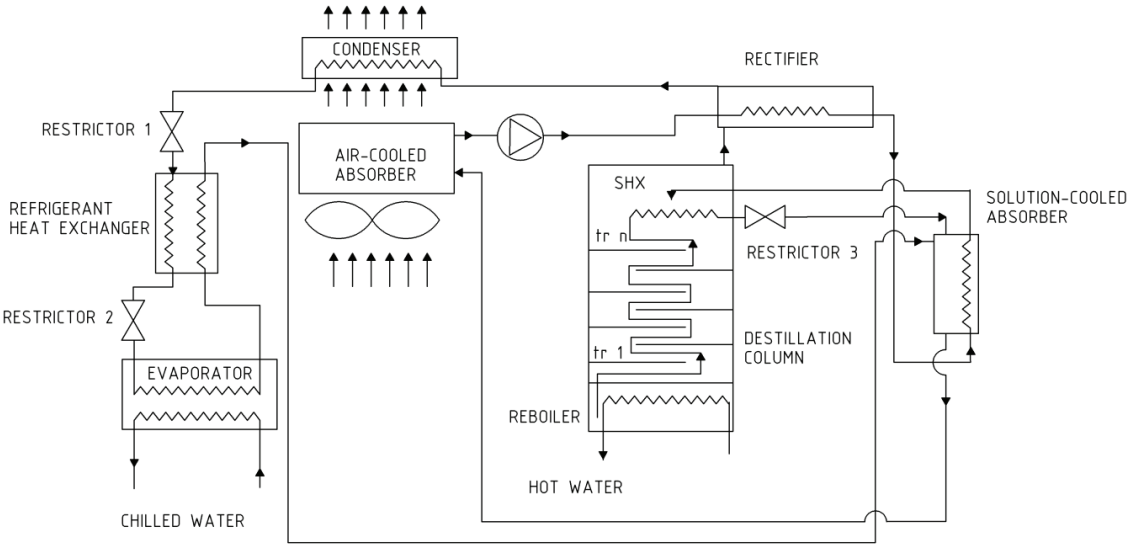

Figure. 1: Schematic diagram of the ammonia-water absorption chiller ROBUR model ACF60-00 LB

The coupling between the absorption and desorption processes is achieved in the solution-cooled absorber (CABS), which operates, on the one hand, thanks to the temperature reduction that occurs in the lean solution flow that leaves the desorber as it passes through the distillation tower (DC), the solution heat exchanger (SHX) and the solution valve (SV), to finally enter the CABS. On the other hand, the rich solution leaving the absorber increases significantly in temperature as it passes through the solution cooled rectifier (CR), until it reaches values close to the dew point temperature of the steam leaving the distillation tower to the rectifier. Therefore, the performance of the absorption system according to a GAX cycle depends on the heat recovery efficiency in DC, SHX and CR.

Condenser, air-cooled absorber, and evaporator tubes are described by its inner diameter, D_i, and thickness, e. The number of tubes is fixed for condenser and absorber, while the tubes length for these devices are obtained in the design process. Conversely, the evaporator tubes length, L, is fixed, while the number of baffles

https://doi.org/10.52202/069564-0081

for the chilled water passage is obtained in the design process. In addition, the refrigerant quality at the exit of evaporator is fixed at 0,96 to limit the temperature glide. It is assumed that both solution-cooled absorber and the solution-cooled rectifier consist of a helical tube. Vapor mass fraction at the rectifier outlet, efficiency of the solution-cooled absorber and the number of turns for both the rectifier and the air-cooled absorber are determined by an iterative process. Nevertheless, while the number of turns remain invariable once are determined, both vapor mass fraction at the rectifier outlet and efficiency of the solution-cooled absorber is determined according to the operational conditions of the chiller. Refrigeration heat exchanger is modeled assuming that its efficiency is 0,9.

The distillation column geometry is defined by its inner diameter D_i, hole diameter, d_h=0,00381 m, tray thickness, e_{tray}, tray spacing, S_t, weir length, l_w, hole pitch, s_h=3 d_h, weir height, h_w. and two relationships, f_1 and f_2 [13], being A_t=π/4 D_i^2, A_d, and A_a=A_t-2A_d, the column area, the downcomer area and the active area, respectively. e_w refers to the weight of the liquid entrainment per unit weight of vapor flowing in the distillation column. The reboiler is assumed to be a cylinder equipped externally with annular fins, with the hot water in cross flow over the cylinder, through the resulting fined annuli passage. The geometry of the finned external surface for condenser, absorber and reboiler annuli, determined by its thickness, t_m, and pitch, s, of their fins are shown in table 1.

Table 1. Chiller geometry.

Condenser/air-cooled absorber		Rectifier/solution cooled absorber		Evaporator	
D_i [m]	0.02	D_{to} [m]	0.075	D_i [m]	0.015
t_m [m]	0.0002	D_{ti} [m]	0.045	e [mm]	0.002
s [m]	0.003	D_{wi} [m]	0.0065	s [m]	1.15(D_i+e)
e [m]	0.002	*e [m]*	0.002	N_{tube}	35
N_{tube}	2			$D_{i,shell}$ [m]	(N_{tube} +1) s
				L [m]	1.1

Reboiler		Distillation column	
h_f [m]	0,63	D_i [m]	0.075
t_m [m]	0,0004	A_d [m^2]	0.12 A_t
s [m]	0,003	S_t [m]	0.15
		h_w [m]	0.1 S_t
		e_{tray} [m]	0.003
		A_d/A_t	$f_1(l_w/D_i)$
		A_h/A_a	$f_2(d_h/s_h)$

2.2. Mathematical models

Mathematical models have been developed for each of the key devices that make up the absorption machine [11]. Such models provide the flow, temperature, concentration of liquid and vapor phases throughout the length of these devices. The following assumptions have been considered:

- Processes are in steady-state
- Heat losses to the ambient are neglected
- Flow is one-dimensional
- Heat and mass transfer is in radial direction of the tube

- Pressure in distillation column, rectifier, solution-cooled absorber, air-cooled absorber, evaporator and condenser is constant

2.2.1 Distillation column

It is assumed that the rectifying section of the distillation column is avoided in the model, due to is low efficiency [3]. Vapor generated in a lower tray interacts with the liquid solution from the upper tray increasing its ammonia content. Simultaneously, the liquid solution coming from the reboiler dissimilates its temperature on its way to the heat exchanger, located at the top of the tower, by interacting with the liquid coming down from the successive trays. For simplicity, the interaction between the liquid coming from the reboiler and the steam generated in each of the trays is disregarded. The ammonia molar fraction of the vapor leaving the i-tray, $\bar{x}_{v,i}$, is obtained calculating the Murphree vapor plate efficiency, e_M. In that way,

$$\bar{x}_{v,i} = \bar{x}_{v,i-1}(1 - e_M) + e_M \bar{x}_{v\,e,i}, \tag{1}$$

where $\bar{x}_{v\,e,i}$, refer to the molar fraction of the vapor leaving the i-tray at thermodynamic equilibrium. The Murphree vapor plate efficiency is obtained as

$$e_M = 6.8 \left(N_{R_e} N_{S_c}\right)^{0.1} \left(N_{D_g} N_{S_c}\right)^{0.115}, \tag{2}$$

here N_{R_e}, N_{S_c}, N_{D_g} are dimensionless groups depending on some thermodynamic properties of the liquid (σ_L, μ_L, ρ_L, D_{kl}, evaluated with the Wilke-Chang expression [13], vapor velocity and geometrical characteristics of the column (fractional free area, A_h/A_t, and weir height, h_w). The effect of the liquid entrainment in the Murphree vapor plate efficiency has also been considered by using the Fair method [13]. The reboiler Murphree efficiency is assumed to be 1. The vapor purification process is eventually completed by partial condensation in the liquid-cooled rectifier. Reboiler is considered as an additional tray. Conservation equations for mass, species and energy in a generic tray are expressed as

$$\dot{m}_{L,F} + \dot{m}_{L,i+1} + \dot{m}_{V,i-1} = \dot{m}_{L,i-1} + \dot{m}_{V,i+1}, \tag{3}$$

$$x_F \dot{m}_{L,F} + x_{L,i+1}\dot{m}_{L,i+1} + x_{V,i-1}\dot{m}_{V,i-1} = x_{L,i-1}\dot{m}_{L,i-1} + x_{V,i+1}\dot{m}_{V,i+1}, \tag{4}$$

$$h_{L,F}\dot{m}_{L,F} + \tilde{h}_{L,i+1}\dot{m}_{L,i+1} + h_{V,i-1}\dot{m}_{V,i-1} + \dot{Q}_{reb} = \tilde{h}_{L,i-1}\dot{m}_{L,i-1} + h_{V,i+1}\dot{m}_{V,i+1}, \tag{5}$$

$$h_{L,i+1}\dot{m}_{L,i+1} + h_{dP,i}\,\dot{m}_{dP} = \tilde{h}_{L,i+1}\dot{m}_{L,i+1} + h_{dP,i+1}\dot{m}_{dP}, \tag{6}$$

$$\left(h_{dP,i} - h_{dP,i+1}\right)\dot{m}_{dP} = \pi D_{wo} e_{tray} h_{t,dP} \frac{(T_{dP\,i} - T_{w0}) - (T_{dP\,i+1} - T_{w0})}{ln\left(\frac{T_{dP\,i} - T_{w0}}{T_{dP\,i+1} - T_{w0}}\right)} \tag{7}$$

where *F* refers to the feed flow, applicable in the feed tray. $\dot{Q}_{reb}$ refers to heat flux supplied by the hot water supply, applicable in the bottom tray. Eq (7) models the heat transfer process that takes place between the dilute solution and the concentrated solution in the gap between consecutive trays. $h_{t,dP}$ refers to the heat transfer coefficient between the dilute solution and the tube wall.

2.2.2 Air-cooled absorber, solution cooled absorber and rectifier

Bulk temperature of the liquid phase, T_{bL}, is obtained by means of mass, species and energy balance at the vapor and liquid interface. Namely, mass balance at interface, which states than the mass transfer between the vapor and the liquid phases must be equal, can be expressed as Eq. (8), where a film model is used. Eq. (9) is obtained stating a balance energy at the liquid vapor interface [7]

$$f_1(T_i, z) = 0, \tag{8}$$

$$f_2(T_i, z) = 0, \tag{9}$$

In these equations, *z* refers to the ratio of ammonia to total molar flux through the interface and T_i is the temperature interface. An iterative process leaves to calculate total and partial mass fluxes transferred through the interface, $\dot{m}$, $\dot{m}_{NH3}$ and $\dot{m}_{H2O}$. New vapor condition is calculated from mass and energy balance in the bulk vapor phase based on the differential control volume, which stablish that

$$d\dot{m}_v = -\dot{m}, \tag{10}$$

https://doi.org/10.52202/069564-0081

$$d(x_{vb}\dot{m}_v) = -\dot{m}_{NH3}, \quad (11)$$

$$d(h_{vb}\dot{m}_v) = -\left(\dot{m}_{NH3} \cdot h_{v,NH3} + \dot{m}_{H2O} \cdot h_{v,H2O} + \dot{q}_{v,i}\right), \quad (12)$$

Similarly, flow rate, temperature and composition of the liquid phase at the exit of the control volume may be obtained with mass balance in the bulk liquid, which states that

$$d\dot{m}_l = \dot{m}, \quad (13)$$

$$d(x_{lb}\dot{m}_l) = \dot{m}_{NH3}, \quad (14)$$

$$d(h_{lb}\dot{m}_l) = -d(h_{vb}\dot{m}_v) - \dot{q}_{cf,i}, \quad (15)$$

The pumped mass flow rate is assumed to be constant, equal to 0,045 kg/s.

2.2.3 Evaporator and condenser

Bulk temperature of the biphasic phase is obtained by means of energy balance

$$h_i\dot{m}_i + h_{cf,i}\dot{m}_{cf} = h_{i+1}\dot{m}_{i+1} + h_{cf,i+1}\dot{m}_{cf}, \quad (16)$$

2.2.4 Reboiler

The energy balance is expressed as

$$h_{L\,2}\dot{m}_{L\,2} + h_{cf,reb\ in}\dot{m}_{cf,reb\ in} = h_{L,1}\dot{m}_{L,1} + h_{cf,reb\ out}\dot{m}_{cf,reb\ out}, \quad (17)$$

where subscripts *L1* and *L2* refers, respectively, to the liquid coming out to the tray 1 and 2 of the distillation column

2.2.5 Heat flux in condenser, air-cooled absorber and reboiler

These devices are externally finned. The heat flux transferred between the coolant and the bulk solution of the discrete element *i*, $\dot{q}_{cf,i}$, is evaluated as

$$\dot{q}_{cf,i} = UA_{cf,i} \cdot DTLM_i, \quad (18)$$

where $UA_{cf,i}$ is the thermal conductance referred to the element outer finned surface, $A_{cf,\,i}$, defined as

$$\frac{1}{UA_{cf,i}} = \frac{1}{h_{Lw}A_{L,i}} + \frac{1}{\eta \cdot h_{cf}A_{cf,i}} + \frac{D_i}{2\,k_w A_{L,i}} ln\left(\frac{D_{w0}}{D_{wi}}\right), \quad (19)$$

$DTLM_i$ is the logarithm mean temperature difference, calculated as

$$DTLM_i = \frac{(T_L - T_{cf\,i}) - (T_L - T_{cf\,i+1})}{ln\left(\frac{T_L - T_{cf\,i}}{T_L - T_{cf\,i+1}}\right)}, \quad (20)$$

η is the overall outer surface efficiency, evaluated as $\eta = 1 - A_{f,i}/A_{cf,i}\left(1 - \eta_f\right)$, where η_f is the fin efficiency and $A_{f,i}$ is the element fin area. In case of the reboiler, only one discrete volume has been considered. The cooling air-facing velocity is fixed at 1,25 m/s

2.2.6 Heat flux in rectifier, solution-cooled absorber and evaporator

The heat flux transferred between the coolant and the bulk solution of the discrete element *i* is evaluated as

$$\dot{q}_{cf,i} = \frac{A_{cf,i}(T_{w0} - T_{cf,i})}{\frac{1}{h_{cf}} + \frac{ln(D_{wo}/D_{wi})}{2k_{w/D_{wi}}}}, \quad (21)$$

where T_{w0} is the temperature of the outer wall of the tube

2.3. Heat and mass transfer coefficients

In the reboiler, the heat transport coefficient between the finned tube wall and the coolant is obtained from [15] and the heat transfer coefficient in the solution side is calculated from Táboas et al. [16], to consider the mass

transfer resistance though the liquid-vapor interface at solution side. The correlation proposed by Klimenko [17] is used between the biphasic refrigerant and the tube surface. In the evaporator, the heat transport coefficient between the tube wall and the coolant is obtained following the procedure described in [18] for the shell-side heat transfer in baffled shell-and-tube heat exchangers. In the condenser and in the absorber, the heat transfer coefficient between the liquid and the tube surface is calculated from the film wise condensation theory in a horizontal tube. In laminar regime, the heat transfer coefficient is obtained from the Nusselt equation for a smooth film [18] ignoring the vapor shear stress effect. The increase in heat transfer due to the waviness of the film flow is considered with the Kutateladze and Gogonin equation [18]. In turbulent regime, the Yüksel and Müller equation [18] has been used to calculate the heat transfer coefficient. Corrections proposed by Numrich equations [18] have been applied to consider the effect of the shear stress at the condensate film surface, both in laminar and turbulent regime. The heat transport coefficient between the solid surface and the coolant for absorber and condenser has been evaluated by [18]. In the absorber, the heat transfer coefficient between the liquid and the liquid vapor interface is assumed to be equal to the heat transfer coefficient between the liquid and the tube wall. The heat transfer coefficient in the refrigerant vapor phase is obtained from Gnielinski [18]. The mass transfer coefficient is calculated by means of the Chilton and Colburn analogy [18] from the heat transfer coefficient.

2.4. Solution method

An iterative process has been implemented to integrate each device that make up the absorption chiller and, thus, to determine the performance of the chiller. It is assumed that the following parameters have fixed values: geometry of the refrigeration system, detailed in Table 1, mass fraction of the solution filled, x_0, quality of the refrigerant at the evaporator outlet, $Q_{evap\ out}$, mass flow rate of the pumped solution, $\dot{m}_{dR}$, air-facing velocity, v_a, and mass flow rate of feed hot water,. Both $N_{turns,\ rect}$ and $N_{turns,\ cabs}$ are fixed values, which must be determined to satisfy all operating conditions. In addition, the mass flow rate of the chilled water, $\dot{m}_{cf,evap}$, may be altered, according to the manufacturer data.

For every operating condition of the absorption system, determined by the ambient temperature and the temperature of the hot water supply, the magnitudes that must be calculated are: the loss of pressure in the valve 1, that participates in determining P_H, and P_L, and thus, the minimum interface area of the condenser and of the air-cooled absorber, x_{ref}, which allows the coupling of the rectifier, eff_{cabs}, which allows the coupling of the solution-cooled absorber, and $\dot{m}_{cf,evap}$, which allows the coupling of the evaporator. The calculation procedure is summarized below.

1. Guess the number of the turns of the rectifier, $N_{turns,\ rect}$
2. Guess the number of the turns of the solution-cooled absorber, $N_{turns,\ cabs}$
3. Guess the los of pressure in valve 1, ΔP_{valv1}
4. Calculate the high-pressure level, P_H, given by ΔP_{valv1} added to the condensation pressure of the saturated refrigerant at ambient temperature
5. Guess the refrigerant mass fraction, x_{ref},
6. Guess the low-pressure level, P_L
7. Guess the refrigerant mass flow rate $\dot{m}_{ref}$
8. Calculate the circulation ratio *f* given by $\dot{m}_{ref}/\dot{m}_{dR}$
9. Calculate the mass fraction of the dilute solution, x_{dP}, given by $\left(f \cdot x_0 - x_{ref}\right)/(f-1)$
10. Calculate the mass fraction of the concentrate solution, x_{dR}, given by $(1-1/f)x_{dP} + x_{ref}/f$
11. Calculate the dilute solution flow rate, $\dot{m}_{dP}$, given by $\dot{m}_{dR} - \dot{m}_{ref}$
12. Calculate the reboil heat flux, $\dot{Q}_{reb}$, the mass fraction, mass flow rate and specific enthalpy of the vapor flow coming out of the upper tray of the distillation column and the temperature of the liquid flow from the reboiler, given by Eqs (1)-(7)
13. Guess the temperature of the solution at the pump outlet, $T_{pump\ out}$
14. Guess the efficience of the solution-cooled absorber, eff_{cabs}
15. Guess the reflux ratio and the mass fraction and temperature of the condensate at the rectifier outlet, T_R and x_R, respectively
16. Check $\dot{Q}_{reb}$ using Eqs (18)-(20). If verified, go to step 17. Otherwise, guess a new value of $\dot{m}_{ref}$ and go to step 8
17. Check the interface area of the evaporator using Eqs (16) and (21). If verified, go to step 17. Otherwise:
    - guess a new value of $\dot{m}_{cf,evap}$, and go to step 17, or
    - guess a new value of P_L and go to step 12

https://doi.org/10.52202/069564-0081

18. Check the reflux ratio and the temperature and mass fraction of the condensate at the rectifier outlet using Eqs (8)-(15). If verified, go to step 19. Otherwise, guess new values of reflux ratio, T_R and x_R and go to step 16
19. Check the number of turns of the rectifier, $N_{turns,\ rect}$ using Eqs (8)-(15) and Eq. (21). If verify, go to step 20. Otherwise, guess a new value of x_{ref} and go to step 9
20. Calculate the refrigerant mass flow rate absorbed in the solution-cooled absorber, $\Delta\dot{m}_{ref,cabs}$, using Eqs (8)-(15) and Eq. (21).
21. Check the number of the solution-cooled absorber, $N_{turns,\ cabs}$, using Eqs (8)-(15) and Eq. (21). Check eff_{cabs}. If verified, go to step 22. Otherwise, guess a new of eff_{cabs} and go to step 15
22. Calculate the interface area of the air-cooled absorber, A_{abs}, using Eqs. (8)-(15) and Eqs. (18)-(20). If the resulting frontal area is greater that of the comercial chiller, guess a new value for ΔP_{valv1} and go to steep 4
23. Check $T_{pump\ out}$. If verified, go to step 24. Otherwise, guess a new value of $T_{pump\ out}$ and go to step 16
24. Calculate the interface area of the condenser using Eqs. (8)-(16) and (18)-(20). If the interface area is greater that a certain máximum value, guess a new value for ΔP_{valv1} and go to steep 4

Table 2 shows input and output parameters of each device to carry out the described iterative process.

Table 2. Iterative process. Input and output parameters.

Distillation column		reboiler		Evaporator	
input	output	input	output	input	output
$\dot{m}_{dR}$, $\dot{m}_{ref}$ x_{dR}, x_{ref}	$x_{v\ upper,}$ $\dot{m}_{v,upper}$ $h_{v,upper}$	$\dot{Q}_{reb}$ $\dot{m}_{cf\ reb}$ $T_{cf\ reb\ in}$	$\dot{m}_{ref}$ $\dot{Q}_{evap}$ COP	x_{ref}, $Q_{evap,\ out,}$ $\dot{Q}_{evap}$ P_L	$L_{eff,\ evap}$
x_R, T_R, $T_{pump,\ out}$ *Reflux ratio*	$\dot{Q}_{reb}$	$x_{v\ bottom,}$ $x_{L\ 2}$ $\dot{m}_{L,2}$		$\dot{m}_{cf\ evap}$ $T_{cf\ evap\ out}$	
ΔP_{valv1}, P_L	$h_{\ dP\ cabs\ in}$	ΔP_{valv1}		$\dot{m}_{ref}$	

rectifier		Solution-cooled absorber		Air-cooled absorber		Condenser	
input	output	input	output	input	output	input	output
$x_{,ref}$ ΔP_{valv1}	$N_{\ turns,\ rect}$	$x_{m,ref,}$ P_L, ΔP_{valv1}	$\Delta\dot{m}_{ref,cabs}$	v_{air}, T_{amb}	$T_{pump,\ out}$	$v_{air,}$ $T_{cf\ out}$ $_{abs,m}$	$L_{eff\ cond}$
$T_{pump\ out,}$ $h_{v\ cond\ in}$	x_R, T_R, x_{ref}, $T_{cf\ out}$ $h_{v\ top}$	$T_{ref\ cabs\ in,}$ $T_{dP,\ cabs\ in,}$ $T_{cf\ cabs\ in}$	$N_{\ turns,\ cabs}$	$\dot{m}_{ref,abs}$, $x_{ref,,cabs\ out}$ $\dot{m}_{L,,abs,in}$, $x_{L\ cabs\ out}$	$L_{eff\ abs}$	ΔP_{valv1} $h_{v\ cond\ in}$	
$x_{dR,}$ $x_{v\ top}$	*Reflux ratio*	$x_{dP,}$ eff_{cabs}		$T_{L,,abs,in}$, $x_{L\ cabs\ out}$		$\dot{m}_{ref}$, x_{ref}	
$\dot{m}_{ref}$, $\dot{m}_{dR}$	$\dot{m}_{v,top}$	$\dot{m}_{dP}$, $\dot{m}_{dR}$	$x_{L\ cabs\ out}$	P_L			

2.4.1. Mathematical model validation

Model has been validated with the data supplied by the manufacturer. Figure 2 compares measured (manufacturer data) and predicted (model), provided that the loss of pressure in valve 1 to be the suitable.

The agreement is fair in the whole range of ambient temperature and of hot feed water analysed. Nevertheless, the validity range of the implemented model cannot be extended to ambient temperatures above 40ºC, as explained below.

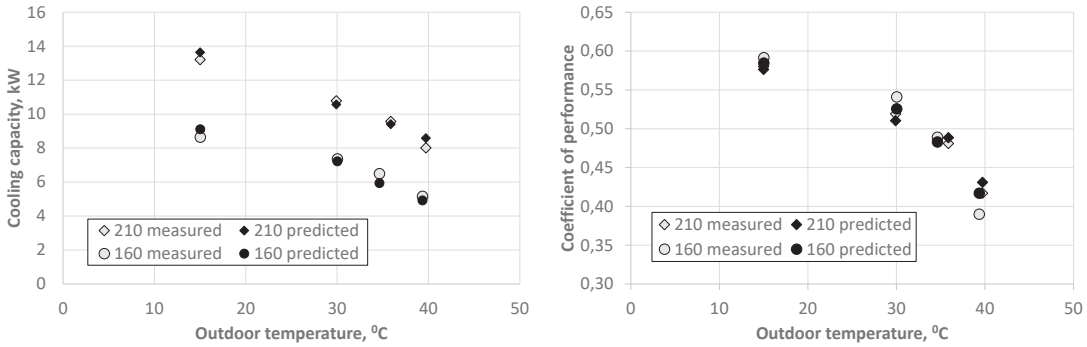

Figure. 2. Measured and predicted values for the performance of the ammonia-water chiller: a) cooling capacity, b) coefficient of performance.

3. Results

Figure 3 depicts shows the effect of the loss of pressure in valve 1 on the high-pressure levels at each operating condition, determined by the feed water temperature and the ambient temperature, ºC. It is observed that, for a certain value of ΔP_{valv1}, P_H increases with ambient temperature as the refrigerant condensing pressure increases. P_H also increases with hot water supply temperature as the mass fraction of the dilute solution decreases.

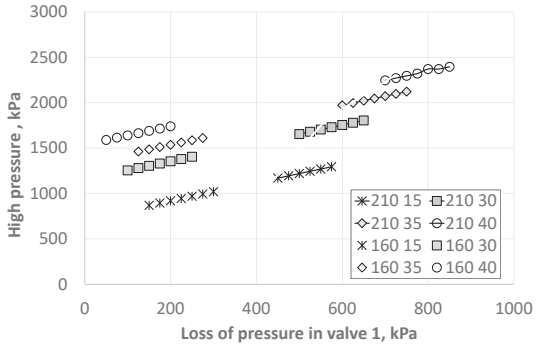

Figure. 3. High-pressure level in the ammonia-water absorption system. Box: feed hot water temperature and ambient temperature, ºC

Figure 4 shows the evolution of the logarithmic mean temperature difference in the condenser, $LMDT_{cond}$, when varying ΔP_{valv1}. The results shows that $LMDT_{cond}$ increases notably when ΔP_{valv1} increases, due to P_H rise. The ambient temperature has also influence on the $LMDT_{cond}$. This is because the condensing pressure of the refrigerant decreases.

It is concluded that the operational limit of an absorption system operating at high ambient temperature and low feed water temperature is established by the size of the air-cooled condenser.

Figure 5 left illustrates the evolution of the low-pressure level, P_L. Results shows that, in all operating conditions, P_L decreases as the ambient temperature drops. This is because P_L is eventually determined by thermal resistance between the refrigerant vapor being absorbed and the coolant-air at the outlet of the air-cooled absorber. Results also show that P_L increases as the temperature of the feed hot water decreases. This is attributable to the influence exerted by the refrigerant mass flow rate, $\dot{m}_{ref}$, as it is explained below.

https://doi.org/10.52202/069564-0081

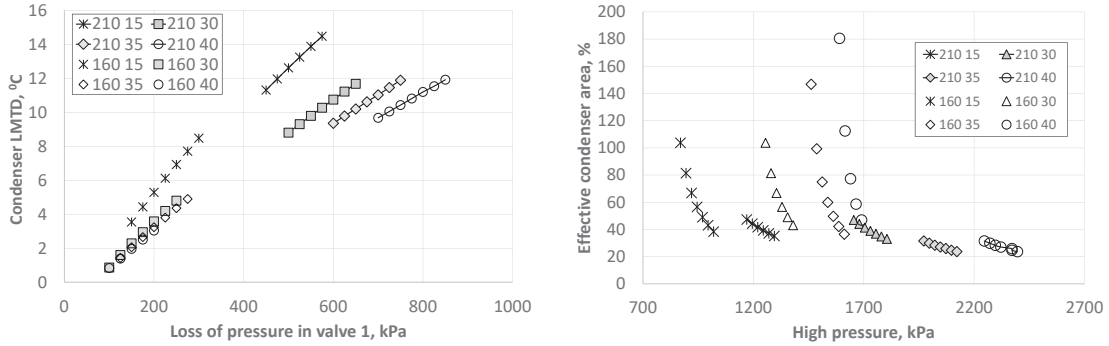

Figure. 4. Condenser: a) logarithmic mean temperature difference, b) Minimum required transfer area, expressed as a percentage of its geometric area. Box: feed hot water temperature and ambient temperature, ºC

Figure 6 left shows the evolution of the cooling capacity, that is, of the refrigerant mass flow rate, with the operating conditions. Figure 6 right illustrates the influence of the temperature of the feed hot water on the logarithmic mean temperature difference of the evaporator, $LMTD_{evap}$. When comparing results in Figure 5 and Figure 6, it can be observed that evaporator coupling results in P_L reduction and $LMTD_{evap}$ increase when $\dot{m}_{ref}$ increases. However, when the temperature of the hot water is 210º C, $LMTD_{evap}$ experiences a slight increase instead when $\dot{m}_{ref}$ is incremented. This is due to, at 210ºC, the rectifier coupling entails refrigerant mass fraction increases as the ambient temperature does, as will see later, what favours $LMTD_{evap}$ increase.

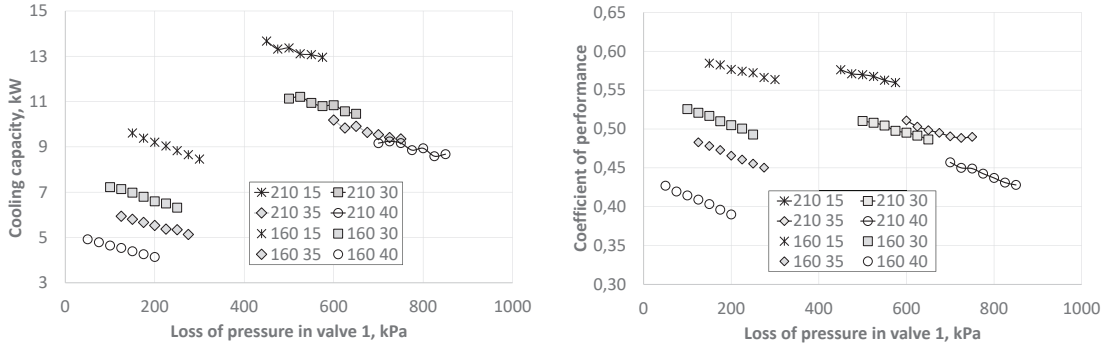

Figure. 5. a) Cooling capacity of the ammonia-water absorption system. b) Coefficient of performance. Box: feed hot water temperature and ambient temperature, ºC.

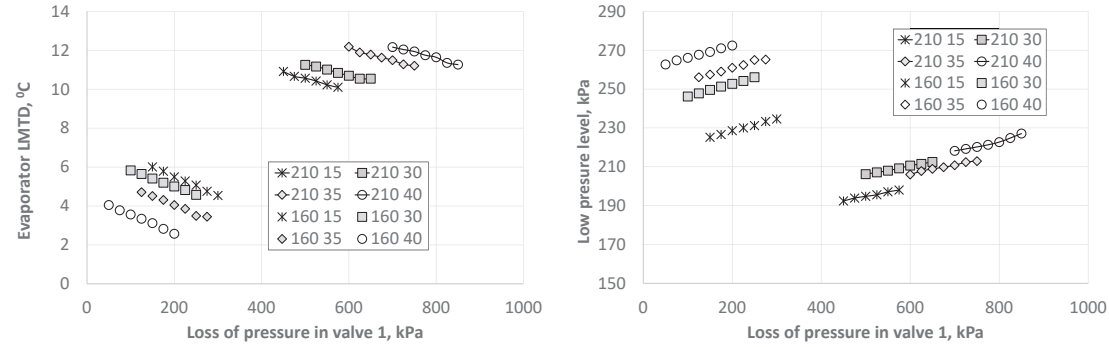

Figure. 6. a) Logarithmic mean temperature difference of the evaporator. b) Low-pressure level. Box: feed hot water temperature and ambient temperature, ºC.

Figure 7 left illustrates the evolution of the effectiveness of the solution-cooled absorber, eff_{cabs}, and the refrigerant mass fraction that allows the coupling of the rectifier and of the solution-cooled absorber. Results

show that eff_{cabs} decreases as the ambient temperature increase when the temperature of the feed hot water is 210ºC. Hence, the temperature of the concentrated solution flow at the CABS outlet reduces, what favours the absorption system to operate as a GAX cycle, even when the ambient temperature is high. In addition, results shows that x_{ref} increases as the ambient temperature increases when the temperature of the feed hot water is 210ºC. This behaviour, particularly noteworthy when the ambient temperature approach to 40ºC, favours COP when the ambient temperature is high.

Figure 7 right shows the influence of the feed water temperature on the minimum area required by the air-cooled absorber, A_{abs}, normalized with the geometric area of the air-cooled absorber. Results show that A_{abs} increases when the temperature of the feed hot water increases. In fact, set the feed water temperature, P_L must be larger than a certain value, which increases as the ambient temperature increases, to assure that A_{abs} remains below the geometric area of the air-cooled absorber. Results show that A_{abs} quickly dismisses when P_L increases. In this sense, since P_L increase as ΔP_{valv1} does, high values of ΔP_{valv1} are preferred when the ambient temperature is high to assure a high cooling capacity. However, reached the maximum value of P_H, a higher ambient temperature entails a reduction of $\dot{m}_{ref}$. Otherwise, $\dot{m}_{ref}$ cannot be absorbed in its entirety.

It is remarkable that, despite the feed water temperature is 210ºC, A_{abs} keeps far from its geometric value when the ambient temperature is 15ºC as compared with that obtained at 30ºC. This behaviour is due to PL is quite similar for both ambient temperatures.

It is concluded that the operational limit of an absorption system operating at high ambient temperature and high feed water temperature is established by the size of the air-cooled absorber.

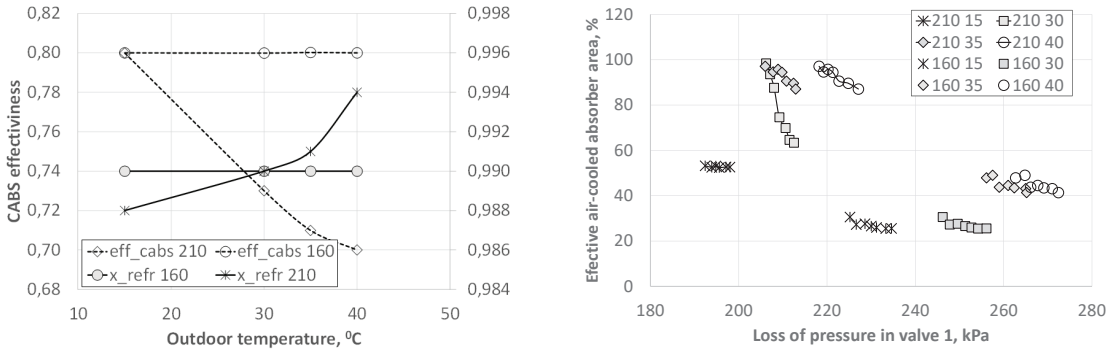

Figure. 7. a) Effectiveness of the solution-cooled absorber. Refrigerant mass fraction. Box: Feed hot water temperature, ºC, b) Minimum required transfer area of the air-cooled absorber, expressed as a percentage of the geometry area

4. Conclusions

In this studio, a detailed analysis of the heat and mass transfer processes that take place in an air-cooled ammonia-water system that operates according to a GAX cycle. The goal is to achieve a detailed inside of the refrigeration system when operates at part load, particularly in hot climates. With that objective, a mathematical model has been developed. The model captures both thermal and mass resistance in the mass and transfer processes that simultaneously occur in the system. The discretized character of the model, with modular structure, together with the consideration of mass transfer resistances gives it a high reliability. The model has been validated with the data of the absorption system manufactured by ROBUR®, model ACF60-00 LB, provided by the manufacturer.

A calculation procedure is presented to evaluate the performance of the cooling system under off-design conditions, when driven by hot water temperature in the range from 160 and 210 ºC and operating in ambient temperature from 15 to 40ºC. It has been assumed that the pumped solution flow rate keeps constant, and the high-pressure level may be used as a control strategy.

Limitations in the operation of the chiller to ambient temperature beyond 40ºC are analysed. Results show that, at high ambient temperature, the cooling capacity of the system when the hot water temperature is 210 ºC is restricted by the size of the air-coolant absorber. On the other hand, difficulties in condenser operation reduce the cooling capacity of the system at high ambient temperature when the feed hot water temperature is 160ºC. At high ambient temperature and high feed hot water temperature, geometry restrictions due to rectifier and to solution-cooled absorber results in high COP, what favours the system operation. However, at such operating condition, the refrigeration system demand for the maximum high-pressure level. Such COP improvement is due to the refrigerant mass fraction increase and efficiency solution-cooled absorber decrease.

https://doi.org/10.52202/069564-0081

Acknowledgement

This work has been developed in the frame of the ASTEP project, funded by the European Union's Horizon 2020 research and innovation program under grant agreement No 884411 and the ACES2030-CM project, funded by the Regional Research and Development in Technology Program 2018 (ref. P2018/EMT-4319)

Nomenclature

Abbreviations

Symbols:

A	area transfer
A_a	active area of the tray, m
A_d	downcomer area
A_h	hole area of the tray, m
A_h/A_t	fractional free area
A_n	net open liquid area of one tray
A_t	tower cross-section area, m^2
CABS	solution-cooled absorber
D_w	wall diameter, m
DLK	diffusivity of the liquid light key
d_h	hole diameter of the tray in the distillation column
e	wall thickness, m
e_{tray}	tray spacing in the distillation column, m
e_M	Murphree vapor plate efficiency
e_w	weight of the liquid entrainment per unit weight of vapor flowing in the distillation column
f	circulation ratio, $\dot{m}_{dR}/\dot{m}_{ref}$
FA	fractional free area
G	superficial mass vapor velocity based on the cross-sectional area of the column
h	reboiler length, m
h	specific enthalpy, kJ/kg
h	heat transfer coefficient
h_f	fin length, m
h_m	mass transfer coefficient
h_w	weir length in the distillation column
l_w	hole pitch of the tray in the distillation column
$\dot{m}$	mass flux
N_{D_g}	dimensionless group, $\sigma_L/\rho_L U_v$
N_{S_c}	dimensionless group, $\mu_L/\rho_L D_{LK}$
N_{R_e}	dimensionless group, $h_w G/\mu_L FA$
P	pressure, kPa
$\dot{Q}$	heat flux
RECT	solution-cooled rectifier
RHX	refrigerant heat exchanger
s	fin pitch, m
S_t	weir length, m
SHX	solution heat exchanger
T	temperature, ºC
t_m	fin thickness, m
V	velocity
x	mass fraction
z	ammonia to molar flux ratio across the vapor-liquid interface

Greek symbols

μ	viscosity, kg/m-s
ρ	density, kg/m^3
σ	surface tension, N/m

Subscripts and superscripts

abs	air-cooled absorber
air	coolant air
cabs	solution-cooled absorber
cond	air-cooled condenser

cf	coupling fluid
dP	dilute solution in ammonia
dR	concentrate solution in ammonia
e	at thermodynamic equilibrium
evap	evaporator
H_2O	water content
H	high level
i	inner
i	interface
L	liquid
L	low level
F	feed of the column distillation
NH_3	ammonia content
o	outer
reb	reboiler
rect	solution-cooled rectifier
ref	refrigerant
V	vapor
¯	molar basis

References

[1] UN United Nations. World Population Prospects — Population Division. Available online: https://population.un.org/wpp/ (accessed on 10 January 2023).

[2] Fernández-Seara J., Sieres J., Vázquez M., Distillation column configurations in ammonia-water absorption chiller refrigeration systems. Int. J. Refrigeration 2003; 26: 28-34

[3] Fernández-Seara J., Sieres J., Vázquez M., Simultaneous heat and mass transfer of packed distillation for ammonia-water absorption refrigeration systems. Int J. Thermal Sciences 2002; 41: 927-935

[4] Fernández-Seara J., Sieres J., Rodríguez C., Vázquez M., Ammonia–water absorption in vertical tubular absorbers. Int J. Thermal Sciences, 2005; 44: 277-288

[5] Fernández-Seara J., Sieres J., Vázquez M., Heat and mass transfer analysis of a helical coil rectifier in an ammonia–water absorption system. Int J. Thermal Sciences 2003; 42: 783-794

[6] Wu S., Eames I.W., Innovations in vapor-absorption cycles. Applied energy 2000, 66: 251-266

[7] Sieres, J., Fernández-Seara J., Modelling of simultaneous heat and mass transfer processes in ammonia-water absorption systems from general correlations. Heat Mass Transfer 2007; 44: 113-123

[8] Killion J.D., Garimella S., A critical review of models of coupled heat and mass transfer in falling-film absorption. Int. J. Refrigeration 2001: 755-797

[9] Ibrahim O.M., Klein S.A., Thermodynamics properties of ammonia-water mixtures. ASHRAE Transaction: Symposia, 1993; CH-93-21-2: 1495-1502

[10] Pereira, J.J., Cabral C.A., Almir C., Batista J., Ochoa A.A., Charamba J.C, Energetic analysis of a commercial absorption refrigeration unit using an ammonia-water mixture. Acta Scientiarum, Technology 2017; 39: 439-448

[11] Klein S.A., A model of the steady-State performance of an absorption heat pump. NBSIR,1982:82-2606

[12] Ng K.C., Tu K., Chua H.T., Gordon J.M., Kashiwagi T., Akisawa A, .Saha B.B, Thermodynamical Analysis of absorption chillers: internal dissipation and process average temperature. Applied Thermal Engineering, 1998; 18: 671-682

[13] Coker A. K., Ludwing's Applied process design for chemical and petrochemical plants. Elsevier, 4th edition; 2010.

[14] Herold K.E., Radermacher R., Klein S.A., Absorption chillers and heat pumps, CRC Press, 2nd edition; 2016.

[15] Kay W.M., A.L. London Compact heat exchangers, McGrawHill, 3rd edition; 1984.

[16] Táboas, F., Vallès M., Bourouis M., Coronas A., Pool boiling of ammonia/water and its pure components: comparison of experimental data in the literature with the predictions of standard. Int. J. Refrigeration 2007; 30: 778-788.

[17] Mills A.F., Transferencia de Calor, McGrawHill, 1st edition; 1999.

[18] VDI Wärmeatlas, VDI Heat Atlas, Springer, 2nd edition, 2010.

https://doi.org/10.52202/069564-0081